SIMULATION IRRADIATION STUDIES ON BCC METALS

Kuramoto, Eiichi
Research Institute for Applied Mechanics, Kyushu University : Associate Professor

Yoshida, Naoaki
Research Institute for Applied Mechanics, Kyushu University : Associate Professor

Tsukuda, Noboru
Research Institute for Applied Mechanics, Kyushu University : Research Associate

Kitajima, Kazunori
Research Institute for Applied Mechanics, Kyushu University : Professor

他

https://doi.org/10.5109/6777093

出版情報：Reports of Research Institute for Applied Mechanics. 28 (90), pp.9-25, 1981-02. 九州大学応用力学研究所
バージョン：
権利関係：

Reports of Research Institute for Applied Mechanics
Vol. XXVIII, No. 90, 1981

SIMULATION IRRADIATION STUDIES ON BCC METALS

By Eiichi. KURAMOTO*, Naoaki. YOSHIDA**, Noboru. TSUKUDA***, Kazunori. KITAJIMA****, Nicholas. H. PACKAN*****
and Lou. K. MANSUR******

4 MeV Ni ion irradiation was performed for pure Fe up to 70 dpa between 350°C and 450°C with and without simultaneous He injection to simulate and understand the irradiation behaviour of ferritic steels in fusion environment. Results were compared with those from electron (HVEM) and proton irradiation. Dislocation density in Ni ion irradiated Fe was 3 times higher than others and dislocations were surrounded by clouds of small defect clusters below 400°C, but at 450°C no such clouds were observed and dislocation density quickly decreased. Voids were observed at 450°C above 20 dpa, showing 0.29 and 0.56% swelling at 70 dpa in dual (Ni and He) and single beam irradiation, respectively. Void density in dual beam irradiation was about twice that in single beam irradiation. Incubation dose for void formation in Ni ion irradiation was about 5 times higher than that in electron irradiation. Attempts were made to interpret these phenomena taking into account heterogeneous production of defects characteristic of ion irradiation, i.e., effects of PKA spectrum and cascades of defects.

Key words: Simulation irradiation, Dual beam, Iron, Void

1. Introduction

High energy heavy ion irradiation has been used in simulation studies of irradiation effects in fusion environment. Especially dual beam irradiation technique gives us very precious informations on the effects of helium on

* Associate Professor, Research Institute for Applied Mechanics, Kyushu University
** Associate Professor, Research Institute for Applied Mechanics, Kyushu University
*** Research Associate, Research Institute for Applied Mechanics, Kyushu University
**** Professor, Research Institute for Applied Mechanics, Kyushu University
***** Researcher, Metals and Ceramics Division, Oak Ridge National Laboratory
****** Researcher, Metals and Ceramics Division, Oak Ridge National Laboratory

development of damage structure in irradiated materials. However, simulation law between charged particle and neutron irradiation, and intercorrelations among various charged particle irradiations have not yet been fully established. It is known that choice of charged particles gives some changes to damage structure in irradiated materials, e. g., proton irradiation usually causes higher void swelling than electron irradiation, which again gives higher swelling than heavy ion and neutron irradiation (1). It is also observed that change of Ni ion energy gives different incubation doses for void formation in 316 S. S. (1).

Recently ferritic stainless steels (HT-9, others) have been rapidly remarked as a candidate of structural material in fusion reactor, because of its low swelling rate and low irradiation creep rate (2-6). Previous studies on void swelling in pure Fe and Mo by HVEM irradiation also showed small void swelling (less than 1%) (7, 8). In the present work Ni ion irradiation was performed in the single and dual beam mode to investigate the damage structure produced by heavy ion irradiation and compare with that produced by electron irradiation. Proton irradiation has also been started to study the effect of incident particle mass on the damage structure. Results will be interpreted by the basic feature of ion induced damage, e. g., cascade of defects and PKA spectrum.

2. Experimental Procedure

MRC MARZ-grade pure Fe was zone-refined in wet H_2 (2 passes), dry H_2 (5 passes) and in vacuum of 10^{-4} Pa (1 pass). The residual resistivity ratio RRR_H of the specimen was about 3500. Specimens for Ni ion irradiation were punched out from a sheet of pure Fe and polished by ♯600 grid paper, 1 μ alumina powder, 0. 5μ diamond powder and 0. 1μ diamond powder successively to obtain a very flat surface. Final size of the specimen was 3mm in diameter and 0. 35 mm thickness. Before irradiation specimens were slightly electrical-polished to remove the layer of polishing damage.

Ni ions were accelerated to 4 MeV by CN Van de Graaff equipped with a Model 910 Physicon ion source in Oak Ridge National Laboratory. ^{58}Ni isotope was mixed with carbon tetrachloride, forming nickel halide and vaporizes near a filament. Only ^{58}Ni ions were selected by velocity filter, and before entrance into 90° magnet charge state was changed into +2 by stripping in a differentially pumped argon gas-filled tube. Beam current of $^{58}Ni^{2+}$ was 1 particle μA. Beam profile was always monitored during irradiation, which had a quite well uniform intensity because of inserting Johnson lens on the beam line. Diameter of $^{58}Ni^{2+}$ beam was about 20 mm and 9 specimens on one holder were able to be irradiated together, but divided into 3 groups by using a mask to study the dose dependence of damage structure. Helium ion was accelerated by the horizontal AN Van de Graaff and injected simultaneously to specimens with Ni ions along a beam line inclined by 15° to that of Ni ions. To make the depth of helium implantation span the region of radiation damage caused by the nickel ions, energy of helium was varied continuously by cycling the terminal voltage from 200 to 400 kV. Details of this dual beam irradiation facility is described in Ref. (9). Irradiation experiments were performed in single and dual beam mode for 3 doses (5, 20, 70 dpa) and 3 temperatures (350, 400, 450°C). Helium appm/dpa ratio was fitted to fusion condition, e. g., ~10, refering to the calculation presented in paper (10).

Electron irradiation was performed by using high voltage electron microscope (HVEM JEM-1000 in Kyushu University). Pure Fe and helium doped Fe specimens were irradiated up to 13 dpa between 300 and 400°C to observe damage structure, especially void swelling, under the condition 1250 kV, 2×10^{-3} dpa/sec in vacuum of 5×10^{-5} Pa. Proton irradiation was performed by using Van de Graaff in Kyushu University. 1 MeV proton beam produces the damage rate 1×10^{-5} dpa/sec at the peak damage, ~7 μm and irradiation was carried out up to 0.1 dpa at 350°C.

Specimens irradiated by Ni ion and proton beam were back-thinned for HVEM observation of damage structure.

3. Experimental Results

In Fig. 1 the profile of damage and implanted helium ions calculated by

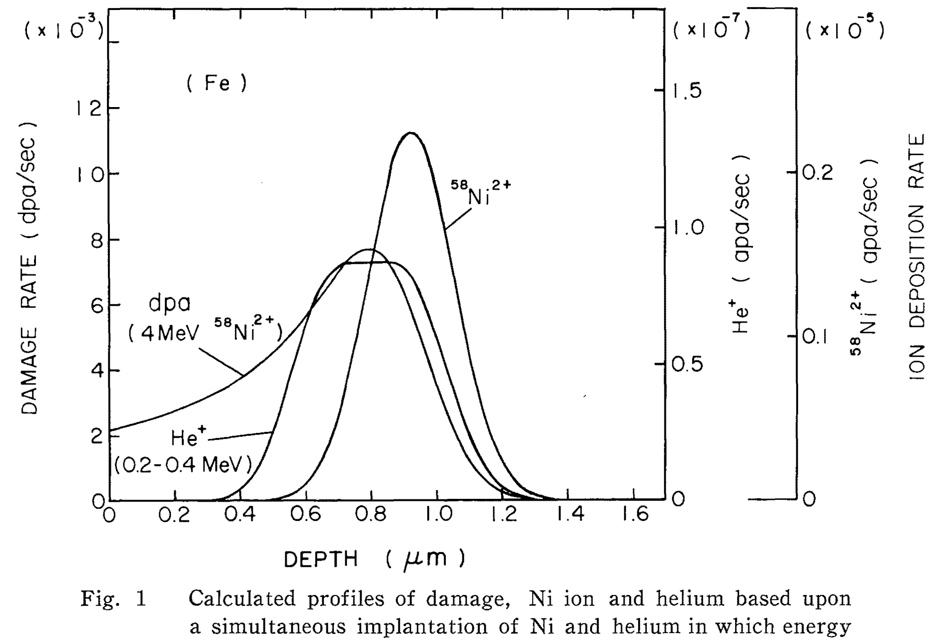

Fig. 1 Calculated profiles of damage, Ni ion and helium based upon a simultaneous implantation of Ni and helium in which energy of helium is sinewave varied between 200~400kV.

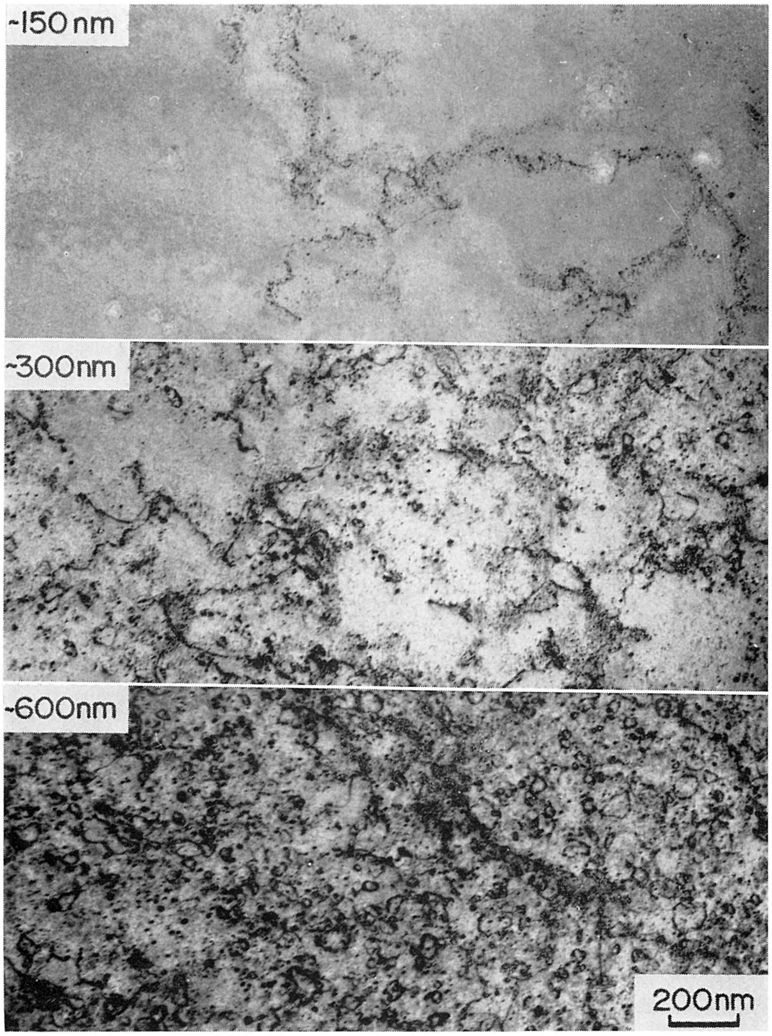

$^{58}Ni^{+2} \rightarrow Fe$, 350°C, 5dpa

Fig. 2 Small defect clusters around dislocation lines in Ni ion irradiated Fe at 350°C up to 5 dp a.

E-DEP-1 code is shown. Ni ions are deposited in the range, 0.7~1.2 μm, so this range is not a pure Fe. The stereoscopic electron microscope observation was carried out in the range between the surface and 0.7 μm depth by using HVEM operated at 500 kV to avoid the additional damage production by HVEM itself.

No voids were observed in Fe specimens irradiated by Ni ions at 350

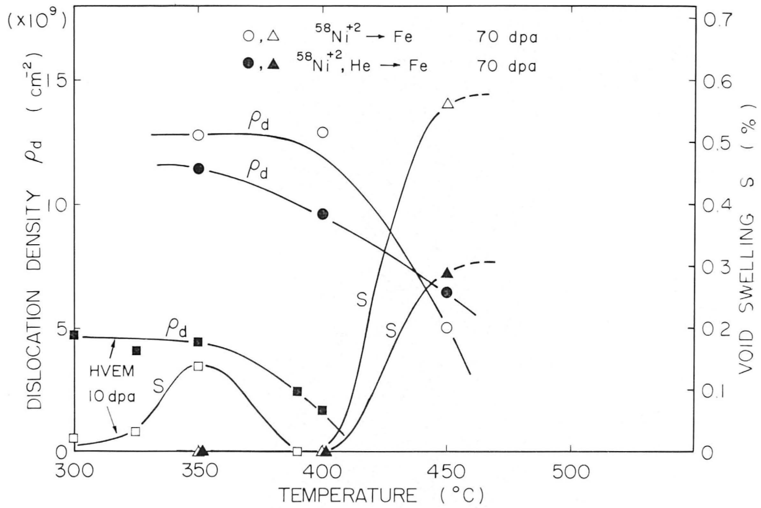

Fig. 3 Temperature dependenece of void swelling in Ni ion irradiated Fe up to 70 dpa. Dislocation density and results in HVEM irradiated Fe are also shown.

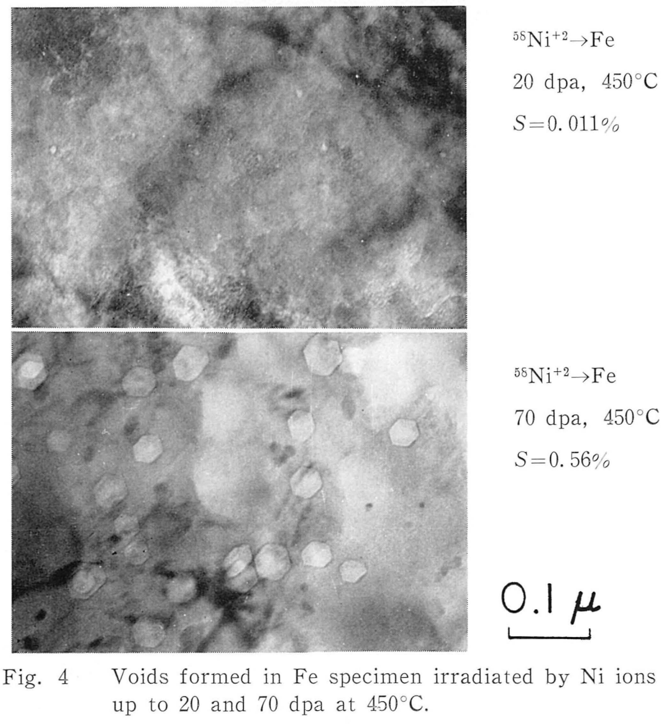

Fig. 4 Voids formed in Fe specimen irradiated by Ni ions up to 20 and 70 dpa at 450°C.

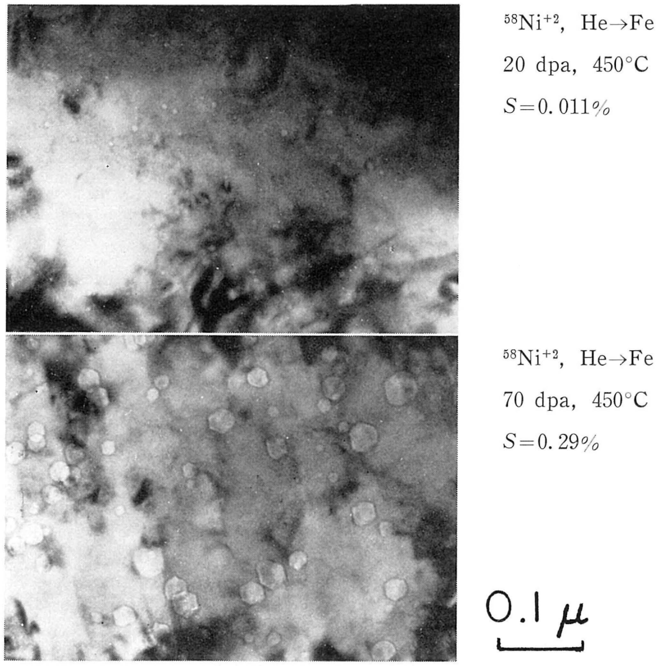

Fig. 5 Voids formed in Fe specimen irradiated by Ni ions with He up to 20 and 70 dpaat 450°C.

and 400°C up to 70 dpa and in these cases dislocations of high density, 1.2 $\times 10^{10}$cm^{-2} were observed. It was characteristic to the case of ion irradiation that dislocations were surrounded by clouds of small loops of point defects as shown in Fig. 2. At 450°C voids were observed at 20 and 70 dpa, and in these cases dislocation density was reduced to$\sim 5\times 10^9$ cm^{-2}, where small loops around dislocations observed at low temperatures disappeared and dislocations take more smooth line shape. Void swelling behaviours are shown in Fig. 3 with the results in HVEM-irradiated pure Fe. There seems 100°C difference in void swelling temperature between Ni ion and electron irradiation in spite of small damage rate difference (5×10^{-3} dpa/sec in Ni ion and 2×10^{-3} dpa/sec in HVEM). Unfortunately we have no data at 500°C, but taking into account a rapid decreasing tendency of dislocation density above 400°C in Ni ion irradiated specimens, void swelling at 500°C may be smaller than those at 450°C. The effect of helium coimplantation (dual beam irradiation) is rather decreasing the void swelling at 450°C, but the void density was increased from 3.0×10^{14} cm^{-3} to 5.4×10^{14} cm^{-3}. Voids observed at 450°C are shown in Figs. 4 and 5 and size distributions are shown in Figs. 6 and 7 for single and dual beam irradiation, respectively. Voids in dual beam irradiated specimen are distributed

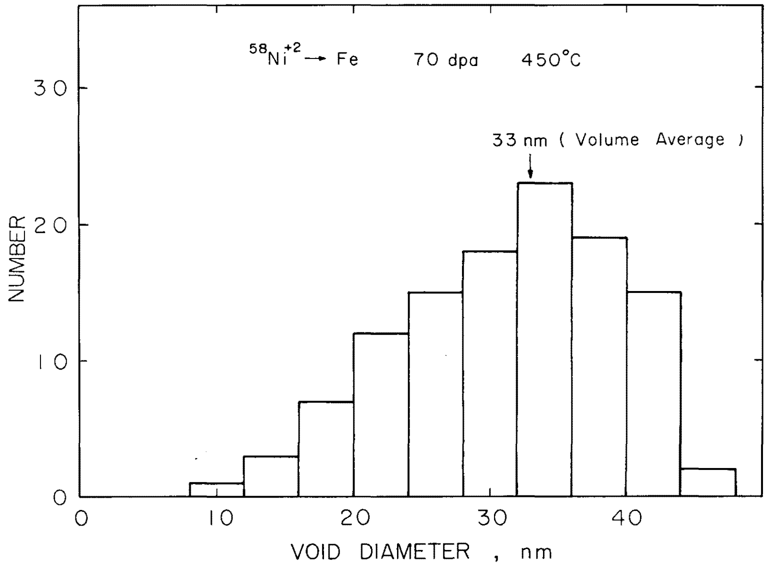

Fig. 6 Void size distribution in Fe specimen irradiated by Ni ions up to 70 dpa at 450°C.

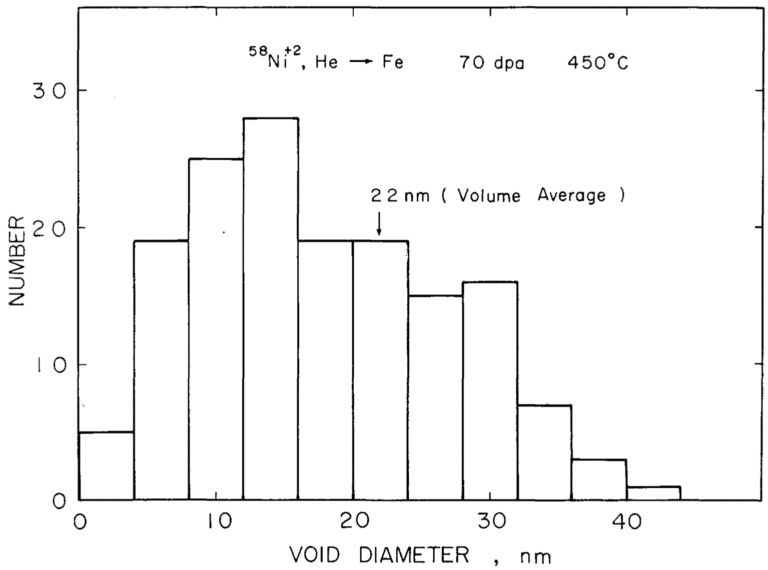

Feg. 7 Void size distribution in Fe specimen irradiated by Ni ions with He up to 70 dpa at 450°C.

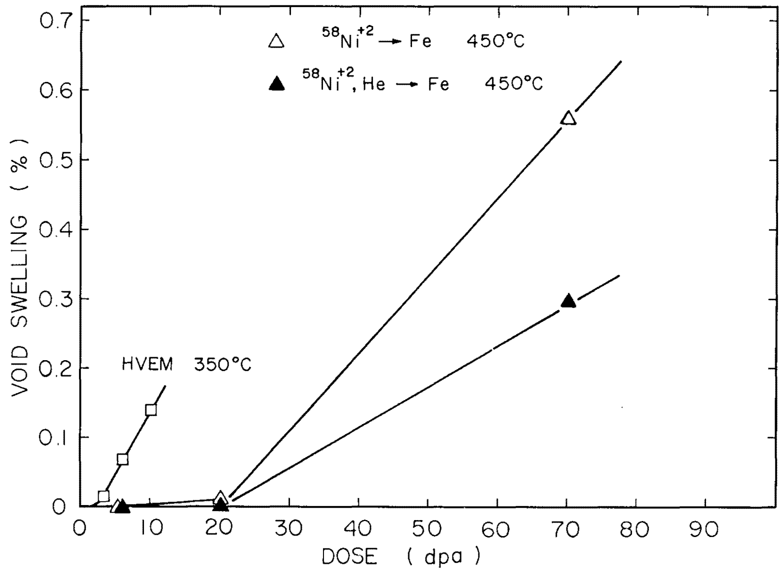

Fig. 8 Dose dependence of void swelling in single and dual beam irradiated Fe. Results in HVEM are also shown.

Table 1. Damage Structure in Single and Dual Beam Irradiated Fe

	350°C	400°C	450°C
5 dpa (single)	$\rho_d=9.6\times10^9$cm^{-2} no voids	$\rho_d=1.1\times10^{10}$cm^{-2} no voids	$\rho_d=1.1\times10^9$cm^{-2} no voids
5 dpa (dual)	$\rho_d=1.0\times10^{10}$cm^{-2} no voids	$\rho_d=8.9\times10^9$cm^{-2} no voids	$\rho_d=1.8\times10^9$cm^{-2} no voids
20 dpa (single)	$\rho_d=8.2\times10^9$cm^{-2} no voids	$\rho_d=6.4\times10^9$cm^{-2} no voids	$\rho_d=4.3\times10^9$cm^{P2} $\rho_v=4.3\times10^{14}$cm^{-3} $\Delta V/V-\Delta V=0.011\%$, $D=8.0$nm
20 dpa (dual)	$\rho_d=1.1\times10^{10}$cm^{-2} no voids	$\rho_d=4.3\times10^9$cm^{-2} no voids	$\rho_d=1.1\times10^9$cm^{-2} $\rho_v=7.1\times10^{14}$cm^{-3} $\Delta V/V-\Delta V=0.011\%$, $D=6.7$nm
70 dpa (single)	$\rho_d=1.3\times10^{10}$cm^{-2}* no voids	$\rho_d=1.3\times10^{10}$cm^{-2} no voids	$\rho_d=5.0\times10^9$cm^{-2} $\rho_v=3.0\times10^{14}$cm^{-3} $\Delta V/V-\Delta V=0.56\%$, $D=33.1$nm
70 dpa (dual)	$\rho_d=1.1\times10^{10}$cm^{-2}* no voids	$\rho_d=9.6\times10^9$cm^{-2} no voids	$\rho_d=6.4\times10^9$cm^{-2} $\rho_v=5.4\times10^{14}$cm^{-3} $\Delta V/V-\Delta V=0.29\%$, $D=21.8$nm

* Arrayed structure of dislocations

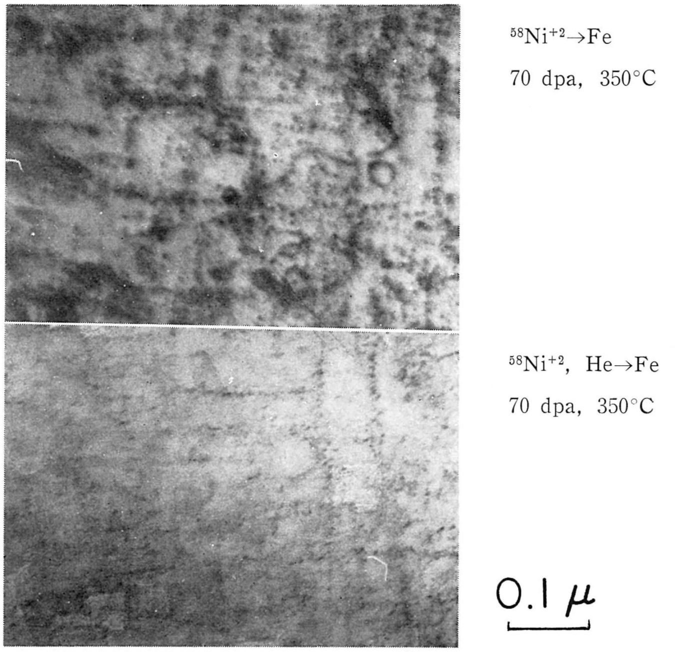

Fig. 9 Arrayed structure of dislocations in Fe specimen irradiated in single and dual beam mode at 350°C up to 70 dpa.

to small sizes (average is 22 nm), but those in single beam irradiated specimen are larger (average is 33 nm). Void swelling at 450°C in single and dual beam irradiated Fe specimens were 0.56 and 0.29% at 70 dpa, respectively.

Fig. 8 shows the dose dependence of void swelling of single and dual beam irradiated Fe together with that of electron-irradiated Fe. Most striking difference between Ni ion and electron irradiation appears in the incubation dose, namely, about 20 dpa in the former and 4 dpa in the latter. The swelling rates in Ni ion irradiation are not so high as compared with that in electron irradiation. The swelling rate in dual beam irradiation is smaller than that in single beam irradiation at 450°C.

All the results are summarized in Table 1. At 350°C and 400°C dislocations of high density are usually induced by single and dual beam irradiation as mentioned above and arrayed structures of dislocations are observed in Fe specimens irrdiated up to 70 dpa at 350°C, especially in dual beam irradiated specimens as shown in Fig. 9. Proton irradiation up to 0.1 dpa at 350°C introduced only dislocations of $3 \sim 6 \times 10^9\ cm^{-2}$ to pure Fe specimens.

4. Discussions

4.1 Theoretical base for nucleation and growth of voids.

Nucleation of void under homogeneous irradiation has been extensively studied from the theoretical view points by Russell (11–14) and Wiedersich (15). According to their theories, nucleation rate of voids J_k can be calculated as a solution of kinetic equations for hierarchy of vacancy clusters, embryos, under the assumption of homogeneous and steady state, and is given as a following expression if supersaturation of vacancy C_v/C_v^e and flux bias D_iC_i/D_vC_v are determined.

$$J_k=Z'\beta_k\rho_k', \tag{1}$$

$$Z'=\left[\frac{-1}{2\pi kT}\left(\frac{\partial^2 \varDelta G_n'}{\partial n^2}\right)\right]^{1/2}_{n_k'},$$

$$\frac{1}{kT}\left(\frac{\partial^2 \varDelta G_n'}{\partial n^2}\right)_{n_k'}=\left\{\left[\frac{1}{kT}\ \frac{\partial^2 \varDelta G_n{}^0}{\partial n^2}\right]\left[\exp\left(\frac{1}{kT}\ \frac{\partial \varDelta G^0}{\partial n}\right)\right]\right\}_{n_k'}$$

$$\rho_k'=N_0\exp(-\varDelta G_k'/kT),$$

$$\varDelta G_n{}^0=-\mathrm{n}kT\ln\left(\frac{C_v}{C_v^e}\right)+(4\pi)^{1/3}(3V)^{2/3}n^{2/3}\sigma,$$

$$\frac{\varDelta G_k'}{kT}=\int_0^{n_k'-1}\ln\left[\frac{\gamma_{n+1}+\alpha_{n+1}}{\beta_n}\right]dn,$$

$$\alpha_{n+1}=\beta_n\ \exp\left(\frac{1}{kT}\ \frac{\partial \varDelta G_n^0}{\partial n}\right),$$

$$\beta_n=Z_v^v A n^{1/3}D_vC_v,$$

$$\gamma_n=Z_i^v A n^{1/3}D_iC_i,$$

where k denotes the value at critical size of void embryo, σ is a surface energy, V an atomic volume, N_0 the number of atomic site, $\varDelta G_n^0$ a free energy for cluster of n vacancies under constrained thermal equilibrium system. β_n, γ_n and α_n are absorption rate of vacancy, interstitial and emission rate of vacancy of cluster n. $\varDelta G'$ is apparent free energy of cluster n under irradiation. D_v, D_i, C_v and C_i are the mobility and concentration of vacancy and interstitial atom, Z_v^v and Z_i^v the bias factor of absorption of vacancy and interstitial to embryo.

On the other hand, growth of void after nucleation is given by the equations, and C_i and C_v can be obtained assuming a steady state under irradiation.

$$\frac{dC_i}{dt}=P-k_i^2D_iC_i-\alpha C_iC_v=0, \tag{2}$$

$$\frac{dC_v}{dt}=P'-k_v^2D_vC_v-\alpha C_iC_v=0,$$

$$P' = (1-\varepsilon)P + D_v C_v^e \{\bar{Z}_v^d \rho_d + 4\pi r \rho_v \exp(-(P_g - 2\sigma/r)\Omega/kT)\},$$
$$k_i^2 = \bar{Z}_i^d \rho_d + 4\pi r \rho_v + C_s,$$
$$k_v^2 = \bar{Z}_v^d \rho_d + 4\pi r \rho_v + C_s,$$
$$\left.\begin{array}{l} C_i = (D_v k_v^2/2\alpha)[\{(1+\mu)^2+\eta\}^{1/2} - (1+\mu)] \\ C_v = (D_i k_i^2/2\alpha)[\{(1+\mu)^2+\eta\}^{1/2} - (1-\mu)] \end{array}\right\},$$
$$\eta = 4\alpha P/D_i D_v k_i^2 k_v^2,$$
$$\mu = (P'-P)\eta/4P,$$

where P and P' are the production rate of free interstitials and vacancies, k_v^2 and k_i^2 are sink strength for vacancies and interstitials, respectively, $\bar{Z}_v^d$ and $\bar{Z}_v^d$ are mean bias factor of absorption of vacancies and interstitials to dislocations, ρ_d and ρ_v are density of dislocations and voids, respectively. Void swelling rate is then calculated by a following expression:

$$\dot{S} = 4\pi r \rho_v (D_v (C_v - \overline{C_v^e}) - D_i C_i), \qquad (3)$$
$$\overline{C_v^e} = C_v^e \exp(-(P_g - 2\sigma/r)\Omega/kT).$$

Effects of cascade is taken into account through the parameter ε, which is interpreted as the fraction of vacancy loss associated with the cascade (16).

On the other hand, both processes of nucleation and growth of voids can be approximated by the Fokker-Planck equation in n space as shown by Wolfer (17, 18).

$$\frac{\partial}{\partial t}\rho_n = -\left(\frac{\partial}{\partial n}F_n - \frac{\partial^2}{\partial n^2}D_n\right)\rho_n + P_n, \qquad (4)$$

$$J_n = \left(F_n - \frac{\partial}{\partial n}D_n\right)\rho_n,$$
$$F_n = \beta_n - \alpha_n - \gamma_n,$$
$$D_n = (\beta_n + \alpha_n + \gamma_n)/2.$$

In the steady state, the region where $F_n > 0$ corresponds to the growth of voids. Void nucleation corresponds to the region $F_n < 0$, and $F_n = 0$ gives a critical size of nucleus of void. From the condition J_n=const.,

$$\Delta G_n'/kT = -\int_1^n dn F_n/D_n,$$

$$J_n* = D_1\rho_1 \Big/ \int_1^\infty dn \quad \exp(\Delta G_n'/kT),$$

which is equivalent to the expression in eq. (1) given by Russell. Wolfer (17) emphasized the bias effect in absorption of interstitial to void embryo, *i.e.* $Z_i^v/Z_v^v>1$ for small n in γ_n and β_n, due to image force on interstitial caused by free surface of embryo.

Extension of the equation to the case of heterogeneous production of point defects can be made in the following way, details of which will be published in another paper (19).

At first, a model process of decay of a cascade for a given PKA energy can be solved using a kinetic equations for clusters in inhomogeneous field. The solution gives the distribution and its time change of free vacancy and interstitial together with those of residual clusters of them. Then the effect of cascades on the development of clusters of n vacancies, prexisting embryo of voids, can be given by the statistical integration of time and space distribution of cascades. Denoting Δt as the effective interval of correlation time we can calculate the first and second moments, $\tilde{F}_n$ and $\tilde{D}_n$, of $\Delta n=n'-n$ from the transition probability $\Psi(n', n; t+\Delta t, t)$, the transformation probability of the cluster n at the time t to the cluster n' at the time $t+\Delta t$. The equation (4) is then replaced by

$$\frac{\partial}{\partial t}\rho_n=-\left(\frac{\partial}{\partial n}\tilde{F}_n-\frac{\partial^2}{\partial n^2}\tilde{D}_n\right)\rho_n+\tilde{P}_n. \quad (5)$$

Contribution of cascades consists of the following effects; overlapping of cascade in a very short time, fluctuation of flux of C_v and C_i within the time Δt, mean production rate of free vacancy and interstitial P' and P, and the mean production rate of clusters of vacancies and interstitials for the time $t>\Delta t$. The growth rate of void for large n is given by $dn/dt=\tilde{F}_n$. These relations coincide with eqs. (2) and (3).

4.2. Nucleation of voids near dislocation line in electron irradiated iron.

As reported in the previous paper (10, 11), voids are nucleated preferentialy along an actively climbing dislocation in electron irradiated pure iron. In Fig. 10 calculations of vacancy and interstitial concentration and void nucleation rate of eq. (1) at compression and expansion side of an edge dislocation are shown for Fe at 350°C, where a dislocation is assumed as a perfect sink, where local bias $Z_i^d\simeq 1.40$ is much larger than the mean bias $\bar{Z}_i^d\simeq 1.03$, and does not climb. Void nucleation rate shows a peak near a dislocation line at a compression side because of higher flux bias $1\text{-}D_iC_i/D_vC_v$ though vacancy supersaturation C_v/C_v^e decreases. In this calculation migration energy of vacancy was taken as a small value 0.8 eV suggested by positron annihilation measurement (20). Furthermore large bias of small embryo in absorption of interstitial, Z_i^v, in eq. (1), emphasized by Wolfer (17), limits the site of nucleation to the neighbourhood of edge dislocation. In an actual specimen an edge dislocation makes a climb motion during irradiation and goes away from the void embryos nucleated near dislocation lines. Then void embryos must shrink unless another edge dislocation

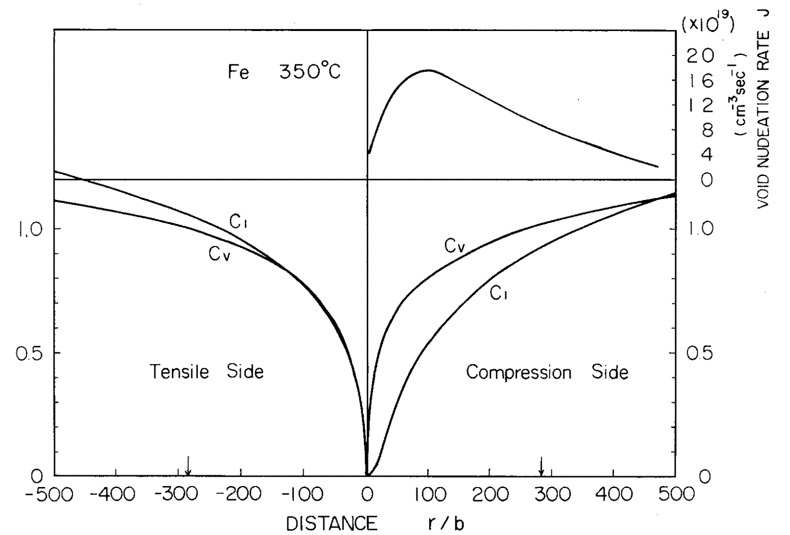

Fig. 10 Calculated void nucleation rate at compression side of an edge dislocation for Fe at 350°C.

approaches to embryo site by climbing and feeds high flux bias field to enhance the growth of embryos. This was the explanation for large dependence of swelling on the dislocation density ρ_d and the narrow temperature range of swelling in pure iron in Fig. 3. Screw dislocations in BCC metals are easy to cross slip and recover at low temperature thus limit the nucleation of voids.

Low swelling and narrow temperature range of swelling reported on ferritic steels (3, 6) may be explained essentially by this characteristic of BCC metals.

4. 3. Effects of cascade on character and density of dislocation.

Compared with that of electron irradiated specimen, the dislocation density in Ni ion irradiated iron is much larger and $\sim 1.3\times10^{10}\mathrm{cm}^{-2}$ as shown in Fig. 3. Furthermore dislocations are surrounded with small clusters of loop type at temperat ure$<$400°C as shown in Fig. 2. These clusters may be vacancy or interstitial type produced by cascades and trapped in the bias field of dislocation. Large dislocation density may be explained by resistance caused by clusters against the movements of dislocations. On the other hand local bias factor Z_i^d may be reduced by presence of clusters, thus limits the nucleation of void at such temperature range.

4. 4. Effects of cascade on nucleation and growth of void.

In Ni ion irradiated specimen, temperature of swelling is about 100°C

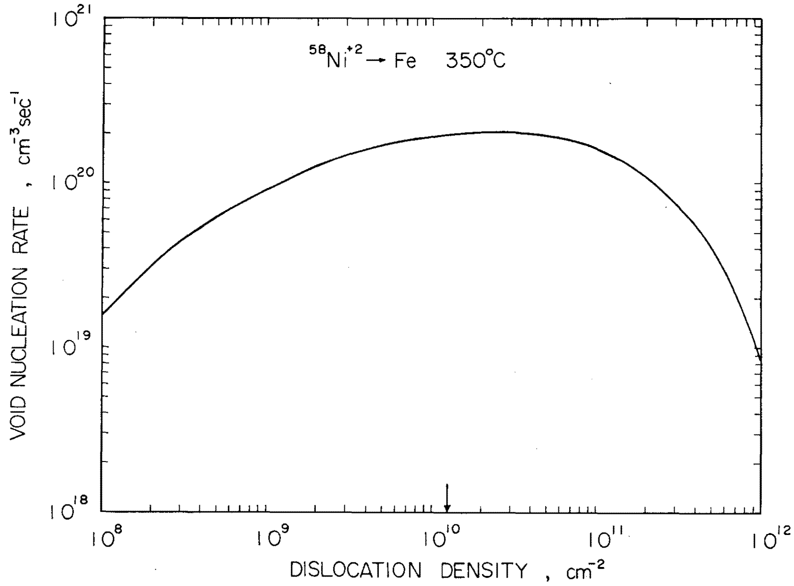

Fig. 11 Calculated void nucleation rate as a function of dislocation density in Ni ion irradiation for Fe at 350°C.

higher than that of electron irradiation, and incubation dose is much larger ~20 dpa than ~3 dpa of electron irradiation. Then what are the main factors in the effects of cascade? High dislocation density solely can not account the problem apart from other factors as shown in Fig. 11, where nucleation rate calculated is shown to be insensitive to ρ_d in the range 10^9~$10^{10}cm^{-2}$, when ε is assumed to be 0. Another important factor is charactor of dislocation described in previous section. Clusters disappeared and void nucleated at 450°C.

Biased production of free point defects, P and P' is another important factor. In Fig. 12 homogeneous void nucleation rate and void swelling rate are calculated as a function of ε under the condition of Ni irradiation for Fe at 350°C. This result shows a very small of amount of ε(0.15%) causes a rapid decrease of both nucleation and swelling rate because of the recombination dominant region at this low temperature. This situation becomes, however, less severe as temperature increases where region changes from recombination dominant to sink action dominant one, which allows occurrence of void swelling at 450°C. Production rate of free defects P is much smaller, by the factor of~0.2 (21), than that used in calculation Fig. 1. This may be the cause of aparent large incubation dose in Fig. 8.

Production of cavity directly from cascade may play another important role. Positron annihilation lifetime measurement is one of the useful techni-

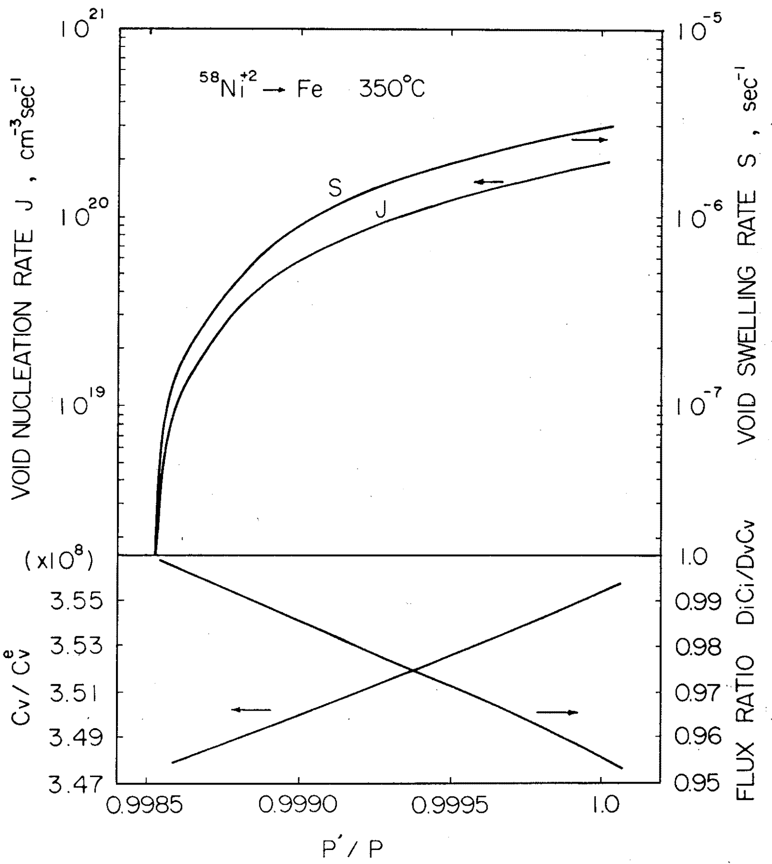

Fig. 12 Calculated void nucleation rate and void swelling rate as a function of ε.

que which gives us some information on the vacancy type clusters formed in the cascades. These clusters can be favorite sites for void nucleation, but number of such vacancy clusters obtained by positron lifetime measurement is usually much smaller than that of cascade by factor of 10^{-2}~10^{-3} (22) even in low dose region of 0.1 dpa.

4.5. Effect of proton irradiation on void nucleation and growth.

As mentioned above Ni ion irradiation is less effective for void formation than HVEM irradiation. On the other hand, it is known that proton irradiation causes larger void swelling than other irradiation method (1). It is considered that in proton irradiation an enhancing factor for void nucleation discussed above is overwhelming a depressing factor. Unfortunately in the present proton irradiation flux was too low (~0.1 dpa) to form voids and only dislocation density was measured ($3\sim6\times10^{9}cm^{-2}$). In the PKA spectrum of proton irradiation fraction of large cascade is much smaller than that in Ni ion irradiation, and fraction of monovacancies vice versa. This feature seems to be related to high void swelling phenomenon in proton irradiation, but detailed experiments and analyses are required.

4.6 Effect of simultaneous helium injection.

As shown in Fig. 3, 8 and Table 1 simultaneous helium injection increases void density but decreases its size, giving rise to smaller void swelling. In stainless steel it is known that helium injection shifts the void swelling region to higher temperature side (23). Unfortunately in the present work we have no data at 500°C, where enhancement of void swelling by simultaneous helium injection may be expected. Moreover, in the present data void observation was performed from the surface to the depth of about 0.7 μm, where the average amount of helium injected is smaller than 10 appm /dpa, value at peak damage, 0.8~0.9μm. Cross sectional viewing method is now being performed to these single and dual beam irradiated specimens.

Acknowledgements

The authors would like to present their cordial thanks to staffs in Research Laboratory of HVEM, Kyushu University for their helps in operation of HVEM and to Dr. M.B. Lewis and Mr. R.A. Buhl for the operation of Van de Graaff.

References

1) Garner, F.A., Powell, R.W., Diamond, S., Lauritzen, T., Rowcliffe, A.F., Sprague, J.A. and Keefer. D.: Radiation Effects Breeder Reactor Structural Materials, Scottsdale, AIME (1977) 543.
2) Smidt, F.A., Jr., Malmberg, P.R., Sprague, J.A. and Westmoreland, J.E.: Irradiation Effects on the Microstructure and Properties of Metals, ASTM STP 611, p. 227.
3) Little, E.A.: J. Nucl. Mat. **87** (1979) 11.
4) Little, E.A. and Stow, D.A.: J. Nucl. Mat. **87** (1979) 25.
5) Paxton, M.M., Chin, B.A., Gilbert, E.R. and Nygren, R.E.: J. Nucl. Mat. **80** (1979) 144.
6) Snykers, M.: J. Nucl. Mat. **89** (1980) 80.
7) Kuramoto, E., Futagami, K. and Kitajima, K.: Proc. 5th Int. Conf. High Voltage Electron Microscope, Kyoto, Japan (1977) 589.
8) Kitajima, K., Futagami, K. and Kuramoto, E.: J. Nucl. Mat. **85** & **86** (1979) 725.
9) Lewis, M.B., Packan, N.H., Wells, G.F. and Buhl, R.A.: Nucl. Inst. Methods **167** (1979) 233.
10) Gabriel, T.A., Bishop, B.L. and Wiffen, F.W.: Nucl. Tech. **38** (1978) 427.

11) Russell. K. C. : Acta Met. 19 (1971) 753.
12) Powell, R. W. and Russell, K. C. : Rad. Effects 12 (1972) 127.
13) Russell, K. C. : Acta Met. 26 (1978) 1615.
14) Maydet, S. L. and Russell, K. C. : J. Nucl. Mat. 82 (1979) 271.
15) Wiedersich, H. : Rad. Effects 12 (1972) 111.
16) Bullough, R., Fyre, B. L. and Krishan, K. : Proc. Roy. Soc. London A 346 (1975) 81.
17) Wolfer, W. G. : Fundamental Aspects of Radiation Damage in Metals, Gatlinburg, Tenn. (1975) 458.
18) Wolfer, W. G. : Breeder Reactor Structural Materials, Scottsdale, AIME (1977) 841.
19) Kitajima, K. Kuramoto, E. and Yoshida, N. to be published.
20) Kuramoto, E., Kitajima, K., Hasegawa, M. ane Koike, S. : Proc. 5th Int. Conf. Positron Annihilation, Lake Yamanaka (1979) 505.
21) Reiley, T. C. and Jung, P. : Radiation Effects Breeder Reactor Structural Materials, Scottsdale, AIME (1977) 295.
22) Kitajima, K., Kuramoto, E. and Hasegawa, M. : Proc. 5thInt. Conf. Positron Annihilation, Lake Yamanaka (1979) 721.
23) Farrell, K. and Packan, N. H. : J. Nucll. Mat. 85 & 86 (1979) 683.

(Received October 31, 1980)